# Combined targeting of lentiviral vectors and positioning of transduced cells by magnetic nanoparticles

Andreas Hofmann[a,1], Daniela Wenzel[b,1], Ulrich M. Becher[c], Daniel F. Freitag[b], Alexandra M. Klein[b], Dietmar Eberbeck[d], Maike Schulte[a], Katrin Zimmermann[a], Christian Bergemann[e], Bernhard Gleich[f], Wilhelm Roell[g], Thomas Weyh[f], Lutz Trahms[d], Georg Nickenig[c], Bernd K. Fleischmann[b,h], and Alexander Pfeifer[a,h,2]

[a]Institute for Pharmacology and Toxicology, [b]Institute of Physiology I, Departments of [c]Internal Medicine II and [g]Cardiac Surgery, and [h]PharmaCenter Bonn, University of Bonn, D-53115 Bonn, Germany; [d]Physikalisch-Technische Bundesanstalt, 10587 Berlin, Germany; [e]Chemicell GmbH, 12103 Berlin, Germany; and [f]Zentralinstitut für Medizintechnik (IMETUM), Technical University Munich, 80333 Munich, Germany

Edited by Inder M. Verma, The Salk Institute for Biological Studies, La Jolla, CA, and approved November 14, 2008 (received for review April 17, 2008)

**Targeting of viral vectors is a major challenge for in vivo gene delivery, especially after intravascular application. In addition, targeting of the endothelium itself would be of importance for gene-based therapies of vascular disease. Here, we used magnetic nanoparticles (MNPs) to combine cell transduction and positioning in the vascular system under clinically relevant, nonpermissive conditions, including hydrodynamic forces and hypothermia. The use of MNPs enhanced transduction efficiency of endothelial cells and enabled direct endothelial targeting of lentiviral vectors (LVs) by magnetic force, even in perfused vessels. In addition, application of external magnetic fields to mice significantly changed LV/MNP biodistribution in vivo. LV/MNP-transduced cells exhibited superparamagnetic behavior as measured by magnetorelaxometry, and they were efficiently retained by magnetic fields. The magnetic interactions were strong enough to position MNP-containing endothelial cells at the intima of vessels under physiological flow conditions. Importantly, magnetic positioning of MNP-labeled cells was also achieved in vivo in an injury model of the mouse carotid artery. Intravascular gene targeting can be combined with positioning of the transduced cells via nanomagnetic particles, thereby combining gene- and cell-based therapies.**

cell positioning | gene transfer | vector targeting

Targeted delivery of viral vectors to specific cell types or certain regions of an organ is an important quest for gene transfer in basic sciences as well as clinical gene therapy (1, 2). Many gene delivery approaches are based on intravascular administration of vectors to achieve transport of the gene of interest to the target site(s). However, physical forces generated by blood flow impede on efficient gene transfer into endothelial cells and counteract retention of viral particles after local administration at specific sites. In addition, ex vivo gene transfer often has to be adapted to the time constraints and temperature (hypothermia) defined by the need to preserve the organ. Short interaction times with the target cells and hypothermia are conditions that are nonpermissive for viral infections (3–5), because they hamper diffusion-limited adsorption of viral vectors to the target cells, which is the first step in the viral entry process. A promising approach to enhance vector particle adsorption is the particles' coupling to magnetic nanoparticles (MNPs) (6–8). Importantly, this approach should also allow for the retention of the MNP–virus particle complexes in the vessel lumen under physiological flow conditions through application of magnetic fields.

Cell-based gene therapy is an important alternative to vector-based delivery of therapeutic genes and gene products to diseased organs. However, cell-based gene therapy and other cell replacement approaches rely on efficient targeting and positioning of genetically modified cells at specific sites within tissues and organs to enable their stable engraftment and restoration of function. In this context, it is an important feature of MNPs that they can be used for magnetic labeling of cells (9–11).

Here, we tested the concept of nanoparticle-mediated selective gene transfer and cell positioning. The use of MNPs coupled to lentiviral vectors (LVs) dramatically enhanced viral gene transfer under nonpermissive conditions, like physiological flow conditions. In addition, altered in vivo distribution of systemically administrated LV/MNP complexes was achieved by application of magnetic fields. Importantly, cells transduced with LV/MNP exhibited magnetic behavior and could be magnetically positioned at specific sites of ex vivo-perfused vessels and in in vivo models of arterial injury.

## Results

**MNP-Assisted Lentiviral Transduction Under Nonpermissive Conditions.** To analyze whether magnetic nanoparticles can enhance lentiviral transduction under nonpermissive conditions, we used HIV-derived LVs carrying a CMV promoter-driven eGFP expression cassette. LV particles were incubated with 2 different kinds of nanoparticles: (*i*) positively charged MNPs [CombiMAG (CM)], which are superparamagnetic nanoparticles with magnetite cores and a coating of strong, positively charged polyethylenimine; and (*ii*) negatively charged MNPs [TransMAG (TM)], with starch as coating and terminal phosphate groups. Initially, we studied virus-binding capacity of these nanoparticles in a range of 2 log-steps (Fig. 1*A*). Both types of MNPs exhibited a similar virus-binding capacity with a maximum capacity of more than 75% within 20 min of incubation (Fig. 1*A*).

In this study we focused on the analysis of MNP-assisted lentiviral transduction under nonpermissive conditions, like hydrodynamic flow forces and low temperature. Both conditions hamper the efficiency of lentivector adsorption to target cells, which is a crucial step in lentiviral infections. First, we focused on MNP-assisted transductions under hydrodynamic flow stress. LV/MNP mixtures were applied to human umbilical vein endothelial cells (HUVECs) while being shaken for 30 min (at room temperature) in the presence of a magnetic gradient field

Author contributions: A.H., D.W., W.R., B.K.F., and A.P. designed research; A.H., D.W., U.M.B., D.F.F., A.M.K., D.E., M.S., and K.Z. performed research; C.B., B.G., T.W., L.T., and G.N. contributed new reagents/analytic tools; A.H., D.W., D.E., B.G., B.K.F., and A.P. analyzed data; and A.H., B.K.F., and A.P. wrote the paper.

The authors declare no conflict of interest.

This article is a PNAS Direct Submission.

[1]A.H. and D.W. contributed equally to this work.

[2]To whom correspondence should be addressed. E-mail: alexander.pfeifer@uni-bonn.de.

This article contains supporting information online at www.pnas.org/cgi/content/full/0803746106/DCSupplemental.

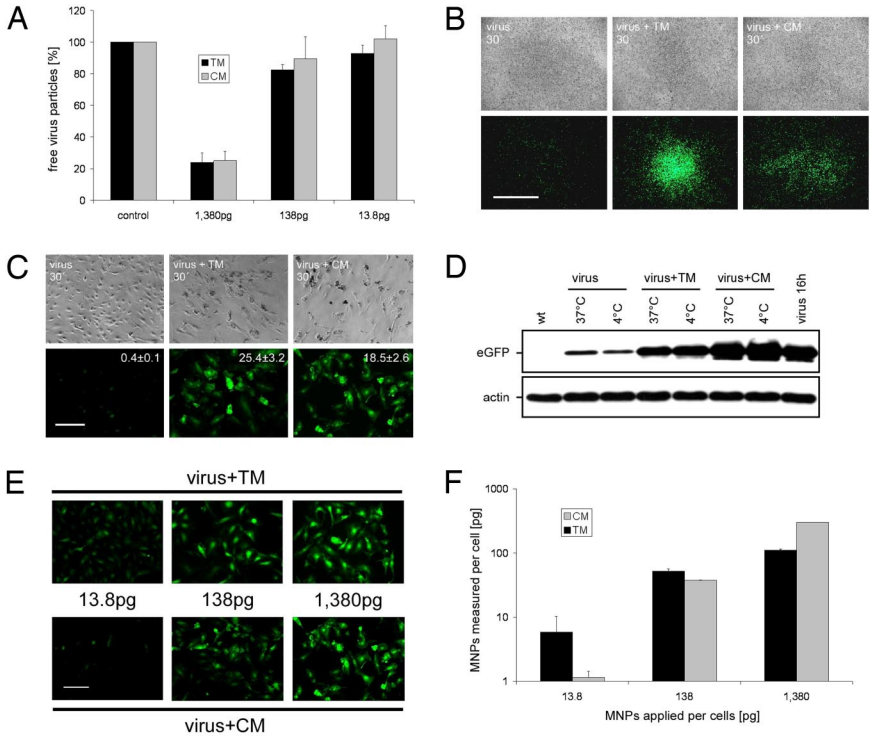


**Fig. 1.** Analysis of transduction efficiency and cellular MNP uptake after MNP-assisted lentiviral infection. (*A*) Analysis of virus-binding capacity of TM and CM nanoparticles. Three different concentrations [1,380 pg of MNPs per 50 virus particles (VPs), 138 pg/50 VPs, and 13.8 pg/50 VPs] were analyzed. Shown are the amounts (±SEM) of unbound virus particles in the supernatants of LV/MNP incubations ($n = 3$). (*B* and *C*) Analysis of transduction efficiency under nonpermissive conditions. (*B*) Transduction of HUVECs under hydrodynamic flow stress (cells were shaken in the presence of a magnetic gradient field). Note that the area of EGFP expression is close to the site of the magnetic gradient field after LV/TM (virus + TM 30′, *Center*) and LV/CM (virus + CM 30′, *Right*) transduction, but not after transduction without MNPs (virus 30′, *Left*). (*C*) Hypothermic transduction (4 °C) of HUVECs with LV/MNP complexes (virus + TM 30′, *Center* and virus + CM 30′, *Right*). Note that under these conditions lentiviral transduction without MNPs (virus 30′, *Left*) achieved only low levels of EGFP expression. The copy number (mean ± SEM) of integrated proviruses per cell ($n = 3$) is indicated in the fluorescence pictures. (*D*) Western blot analysis of EGFP expression after transduction of HUVECs with LVs (virus) or LV/MNP complexes (virus + TM, virus + CM) for 30 min at 4 °C and 37 °C. Overnight-infected cells (virus 16h) were used as control. (*E* and *F*) Analysis of transgene expression and cellular MNP uptake. HUVECs were transduced with equal amounts of lentiviral particles (50 VPs per cell), but different MNP doses (picograms of MNPs applied per cell are indicated). (*E*) Fluorescence images showing transgene expression 3 days after LV/TM (virus + TM) and LV/CM (virus + CM) transduction. (*F*) Quantification of nanoparticle uptake by magnetorelaxometry. Error bars are the uncertainty of the magnetic relaxation signal. (Scale bars: *B*, 5 mm; *C* and *E*, 100 $\mu$m.)

[supporting information (SI) Fig. S1]. Three days after LV/TM and LV/CM transduction, strong eGFP expression was observed in the target area at the site of the magnetic gradient field (Fig. 1*B*). In contrast, transduction without magnetic nanoparticles under the same conditions resulted only in low-level fluorescence, which was detected throughout the whole cell culture plate (Fig. 1*B*).

Next, we analyzed the efficiency of MNP-assisted lentiviral transductions under hypothermic conditions (30 min at 4 °C). Hypothermic transduction of HUVECs with LV/TM and LV/CM complexes resulted in strong EGFP fluorescence (Fig. 1*C*). As expected, transduction without nanoparticles under the same conditions achieved only low levels of transgene expression (Fig. 1*C*). Quantitative real-time PCR analyses of the LV/TM- and LV/CM-transduced HUVECs revealed similar copy numbers per cell (see indices in Fig. 1*C*) as overnight-infected cells (mean ± SEM, 20.19 ± 2.4; $n = 3$). Western blot analysis (Fig. 1*D*) revealed that MNP-assisted LV transduction under hypothermic conditions (4 °C) resulted in (mean ± SEM) 80.2 ± 3.2% (virus + TM) and 110.1 ± 7.4% (virus + CM) transgene expression ($n = 3$) compared with cells infected overnight (virus 16 h) at 37 °C.

To further analyze the efficiency of MNP-assisted transduction under nonpermissive conditions, a broad set of cells from different species was transduced, including primary rat endothelial cells, murine NIH 3T3 fibroblasts, and porcine skin fibroblasts. In all cell lines analyzed, LV/MNP transduction resulted in efficient transgene expression compared with cells transduced in the absence of MNPs (Fig. S2).

**Analysis of Cellular MNP Uptake.** Uptake of LV/TM and LV/CM complexes into endothelial cells was analyzed for 3 different MNP doses (13.8, 138, and 1,380 pg per cell). Transductions with LV/TM (Fig. 1*E Upper*) and LV/CM (Fig. 1*E Lower*) resulted in similar efficiencies, and the levels of transgene expression increased with rising MNP dose (Fig. 1*E*). To quantify MNP uptake, transduced cells were analyzed by magnetorelaxometry; that is, the measurement of the initial amplitude of the MNP magnetization decay (12). The lowest MNP dose analyzed (13.8 pg per cell) resulted in a cellular MNP content of 6 pg per cell and 1 pg per cell for LV/TM and LV/CM, respectively (Fig. 1*F*). The amount of nanoparticles per cell increased to 110 pg per cell (LV/TM) and 300 pg per cell (LV/CM) after 1,380 pg per cell was applied (Fig. 1*F*). We followed the progress of cellular MNP uptake over a time span of 8 h and found perinuclear accumulation of MNPs already 60–90 min after transduction (Fig. S3*A*). In addition, we evaluated the persistence of MNPs by magnetorelaxometry (Fig. S3*B*). The MNP content decreased to 10% (half-life ≈3 days) of the initial MNP content within 9 days after transduction (Fig. S3*B*).

**MNP-Assisted Transduction of Mouse Aortas Under Physiological Flow Conditions.** To study MNP-assisted lentiviral transduction of vessels, aortas were isolated and transduced with LV/MNP ex

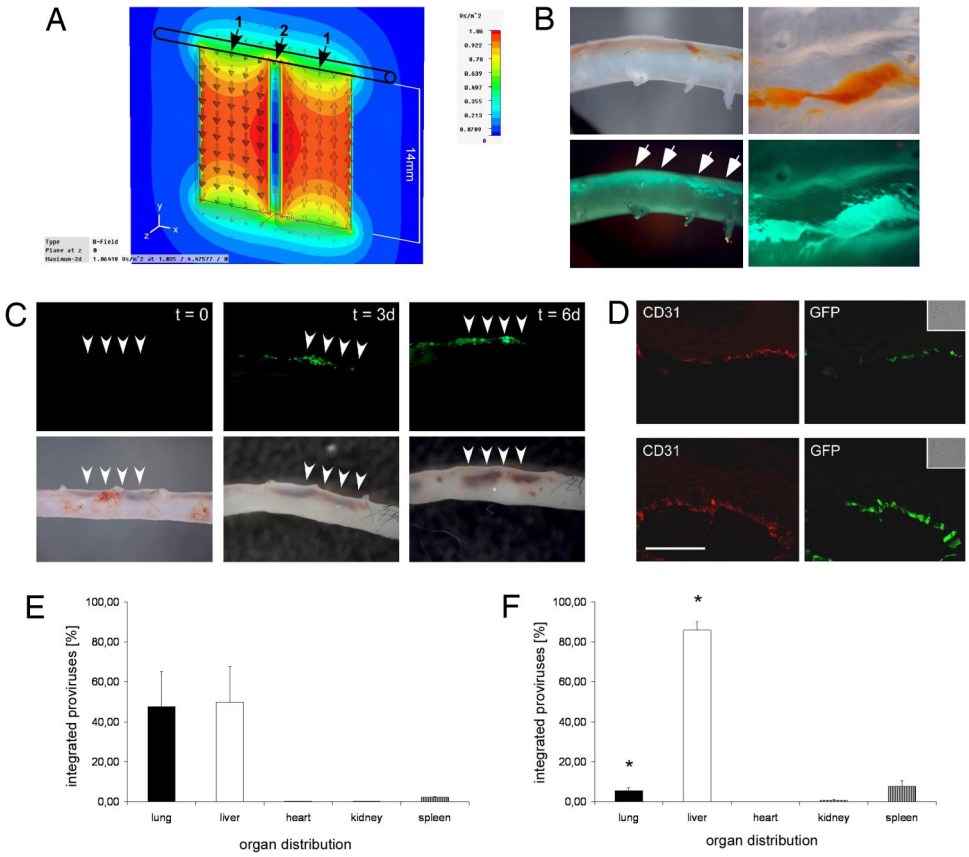


**Fig. 2.** Ex vivo and in vivo targeting of lentiviral vectors by magnetic nanoparticles. (*A*) During ex vivo perfusion, 2 magnets were placed at one side of the aorta. The magnetic flux density of the magnets is shown as a multicolor contour plot in the *x*–*y* plane at $z = 0$ (center plane through the 2 magnets). 1 indicates poles of the magnets; 2, gap between the magnets. (*B*) Ex vivo perfusion of aortas with a mixture of magnetic nanoparticles and fluorescent LV particles containing *gag*-EGFP fusion proteins. Note that directly after perfusion (*Left*), nanoparticles (*Upper*), and EGFP fluorescence originating from the virus particles (*Lower*) were clearly visible at the site of the magnetic field (indicated by the arrows, 3.2× magnification). View of the intima layer after opening of the aorta (*Right*, 8× magnification). (*C*) Aortas were perfused ex vivo for 30 min with LV/CM complexes while magnets were placed at one side of the aorta (indicated by the arrowheads, 3.2× magnification). At the end of the perfusion ($t = 0$), accumulation of LV/CM complexes is clearly visible in the brightfield pictures (*Lower*). Note the EGFP expression after 3 (t = 3d) and 6 (t = 6d) days of culture (*Upper*). (*D*) Immunhistochemical analysis of transgene expression in aortic sections after perfusion with LV/TM (*Upper*) and LV/CM (*Lower*) complexes. EGFP expression is clearly visible in the CD31-positive endothelial layer (red) of the aortas. (*Inset*) Brightfield pictures. (Scale bar: 50 $\mu$m.) (*E* and *F*) In vivo distribution of integrated lentivectors after injection into the carotid artery of mice. Shown is the percental distribution (±SEM) in different organs ($n = 3$) of mice that were exposed to a strong magnetic field at the right abdominal wall (*F*, $n = 5$) and of control mice (*E*, $n = 3$). *, $P < 0.05$ compared with the control group.

vivo. After application of a magnetic gradient field, aortas were washed, cultured for 6 days, and then analyzed for transgene expression. LV transduction for 30 min at 4 °C resulted only in low transgene expression (Fig. S4). In contrast, the use of LV/MNP complexes significantly enhanced transduction efficiency (Fig. S4). LV/TM-transduced aortas as well as LV/CM-transduced aortas showed levels of transgene expression similar to those in overnight-infected tissues (Fig. S4). Thus, magnetic nanoparticles can dramatically increase lentiviral transduction efficiency of vessels under nonpermissive conditions.

Next, MNP-assisted targeting of LVs in intact aortas was studied by using an ex vivo flow-loop system that mimics physiological flow conditions (Fig. S5*A*). Two magnets were placed at one side of the aorta to deflect LV/MNP complexes from their flow orientation by the magnetic flux density gradient (Fig. 2*A*). The absolute magnetic flux density within the aortas (at 0- to 1-mm distance from the magnets) was calculated by means of numeric field simulation (Fig. S5 *B* and *C*). Fluorescent LV particles containing *gag*-EGFP fusion proteins (13) were used to demonstrate retention of LV/MNP complexes (Fig. 2*B*). Using lentivectors carrying the CMV-EGFP reporter cassette, we analyzed transduction of the endothelium. Directly after perfusion, MNP accumulation was clearly visible at the side of the magnets (Fig. 2*C*, $t = 0$). Only 4% of the virus/MNP complexes remained in the flow system after perfusion, indicating high targeting efficiency. Transgene expression in the aortas was followed over 6 days. Both LV/CM (Fig. 2*C*) and LV/TM (data not shown) transductions resulted in EGFP expression at the site of the magnetic gradient field. Histological analysis of aortas perfused with LV/TM (Fig. 2*D Upper*) and LV/CM (Fig. 2*D Lower*) revealed EGFP expression in the intima layer, as demonstrated by colocalization of the endothelial marker CD31 with EGFP. As controls, aortas were perfused with (*i*) LV without MNPs, (*ii*) MNPs without LV, and (*iii*) LV/MNP complexes without a magnetic gradient field. In none of these controls was EGFP expression observed (data not shown).

**MNP-Assisted Transduction of Organs In Vivo—Analysis of Biodistribution.** To analyze whether a magnetic gradient field can alter the native in vivo distribution of LVs, we injected LV/CM complexes via catheter into the carotid artery of mice. The number of viral integrants in different organs was determined by using quantitative real-time PCR, which has a high degree of sensitivity, reproducibility, and accuracy in quantifying LV copy numbers in

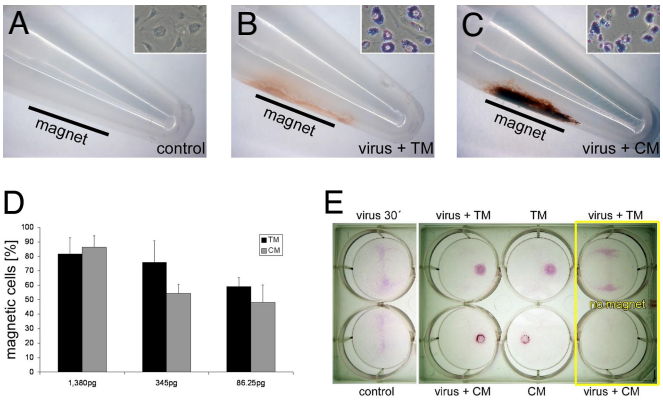


**Fig. 3.** Nanomagnetic cell positioning. (*A–C*) At 24 h after transduction with LV/MNP complexes, HUVECs were transferred into reaction tubes with a magnet placed at one side (indicated by the black bars). Accumulation of cells at the tube walls was seen only for LV/TM-transduced (*B*) and LV/CM-transduced (*C*) cells, but not for control cells (*A*). Prussian blue stainings of the cells (*A–C Insets*) demonstrate MNP incorporation (*Inset*, width ≈35 μm). (*D*) The experiments shown in *A–C* were performed with 3 different MNP doses (1,380 pg/50 VPs, 345 pg/50 VPs, and 86.25 pg/50 VPs). Shown are the numbers (mean ± SEM) of ''magnetic'' cells that adhered to the tube walls ($n = 4$). (*E*) Targeted attachment of HUVECs after transduction with LV/MNP complexes (virus + TM and virus + CM) or with MNPs alone (TM and CM). Shown are the plates after staining with sulforhodamine B dye. Note that directed cell positioning in close proximity to the magnets was observed only for cells that were transduced with nanoparticles (4 wells in the middle). Control, untreated cells; virus 30′, cells transduced without MNPs; no magnet, cells cultured without magnets below the plates.

cells and organs (14–16). Analyses of control mice 6 days after injection of the LV/MNP complexes ($n = 3$) revealed the presence of viral integrants predominately in the lung and liver (Fig. 2*E*). Placement of a permanent magnet at the right abdominal wall close to the liver ($n = 5$) resulted in a significant redistribution of LV/MNP complexes toward the liver and, concomitantly, the number of viral integrants in the lung was significantly reduced (Fig. 2*F*). Thus, application of an external magnetic field can be used to alter the tissue distribution of MNP-coupled LV particles in vivo.

**Positioning of Transduced Cells by Magnetic Fields.** The efficient cellular uptake (Fig. 1*F*) of MNPs should also render the cells superparamagnetic, and therefore allow their magnet-guided positioning. Initially, magnetic retention of LV/MNP-transduced cells was analyzed by transferring them into reaction tubes with a magnet placed at one side of the tubes (Fig. 3 *A–C*). After 15 min, retention of cells close to the magnets was observed for LV/TM-transduced (Fig. 3*B*) and LV/CM-transduced (Fig. 3*C*) cells, but not for untreated control cells (Fig. 3*A*). After transduction with LV/TM and LV/CM at the highest MNP dose (1,380 pg of MNPs applied per cell), more than 80% of the transduced cells were retained by the magnetic gradient field (Fig. 3*D*). Next, we analyzed whether LV/MNP-transduced cells can be positioned in the presence of hydrodynamic flow forces. HUVECs were transduced with and without MNPs, transferred to 6-well plates, and cultured while slowly being shaken, with magnets positioned under the plates (Fig. S1). As additional controls, LV/TM- and LV/CM-transduced cells also were cultured without magnets below the plates. After 24 h of culture, cells on the plates were stained with sulforhodamine B (Fig. 3*E*). In contrast to control cells, LV/MNP-transduced cells (virus + TM and virus + CM) and cells transduced with MNPs alone (TM and CM) were retained in the areas above the magnets (Fig. 3*E*). These findings clearly indicate that superparamagnetic nanoparticles can be used to position cells by a magnetic gradient field even in the presence of hydrodynamic forces.

**Positioning of Transduced HUVECs to the Intima Under Physiological Flow Conditions.** Next, we studied whether LV/MNP-transduced cells can be positioned to vessel walls; that is, to the native endothelial cell layer. Because we observed higher cell seeding efficiencies and lower adverse effects on cell viability for LV/TM compared with LV/CM-transduced cells (Fig. S6), we used these MNPs for the following experiments. Aortic strips were incubated with LV/TM-transduced HUVECs while slowly being shaken to induce hydrodynamic forces. After 24 h, strong EGFP fluorescence was observed in aortas cultured in the presence of a magnetic gradient field (Fig. 4*A Left*). Aortas that were cultured without a magnet exhibited only marginal EGFP expression (Fig. 4*A Right*). The histological analysis using antibodies against human CD31 [platelet endothelial cell adhesion molecule-1 (CD31h)] demonstrated that cells positive for EGFP and human CD31 were found at the luminal surface of the vessel (Fig. 4*B*), indicating successful positioning of the transduced HUVECs to the intima layer. A detailed analysis of the fluorescent signals revealed that almost 100% of the EGFP signal was colocalized with human CD31.

To study MNP-assisted cell positioning under more physiological conditions, we used our flow-loop aortic perfusion system (Fig. S5*A*). During the perfusion, more than 60% of the LV/TM-transduced cells were retained at the intima of the aorta in the presence of a magnetic gradient field (Fig. 4*C*). Immunohistochemical staining of the perfused aortas with antibodies against human and murine CD31 revealed that the EGFP signals were colocalized with human CD31 (Fig. 4*D*). Detailed image analyses revealed a 93% overlap between EGFP and CD31h signals. Interestingly, both signals were located in the endothelial layer (murine CD31) of the aorta (Fig. 4*D*). These findings demonstrate that LV/MNP-transduced cells can be positioned to the endothelial layer of perfused vessels.

**Positioning of Endothelial Cells to Injured Vessels In Vivo.** To demonstrate the utility of the technology in vivo, we first studied positioning of MNP-labeled cells in noninjured murine vessels. LV/TM-transduced HUVECs were injected into the thoracic aorta (via a catheter) of mice. Small magnets were positioned close to the abdominal aorta or iliac artery. In vessels that were subjected to a magnetic field, we found strong EGFP fluorescence (derived from the LV/MNP-transduced HUVECs) in the areas that were located close to the magnets (Fig. S7), indicating that intravascular cell positioning by magnetic force is feasible in vivo.

To evaluate the feasibility of our approach in a more clinically relevant setting, we used an in vivo injury model of the mouse carotid artery (17). Our aim was to position superparamagnetic endothelial cells to the denuded common carotid artery (CCA). For this purpose, 40,000 LV/TM transduced HUVECs were infused via the external carotid artery while small magnets were positioned at the injured CCA. In parallel, control experiments were performed under the same conditions without placing a magnet to the CCA. Retention of MNP-labeled, transgenic HUVECs was analyzed by fluorescence stereomicroscopy (Fig. 4*E*) and histology (Fig. 4*F*). Importantly, fluorescence imaging revealed EGFP expression at the injured vessel walls in the presence of magnets (Fig. 4*E*, *Left*), but not in control mice (Fig. 4*E*, *Right*). Histological analysis corroborated the presence of MNP-labeled, EGFP-expressing cells at the site of the magnetic gradient field (Fig. 4*F*). Taken together, MNP-labeled cells can be positioned to the vessel wall in vivo by magnetic force at sites of arterial injury.

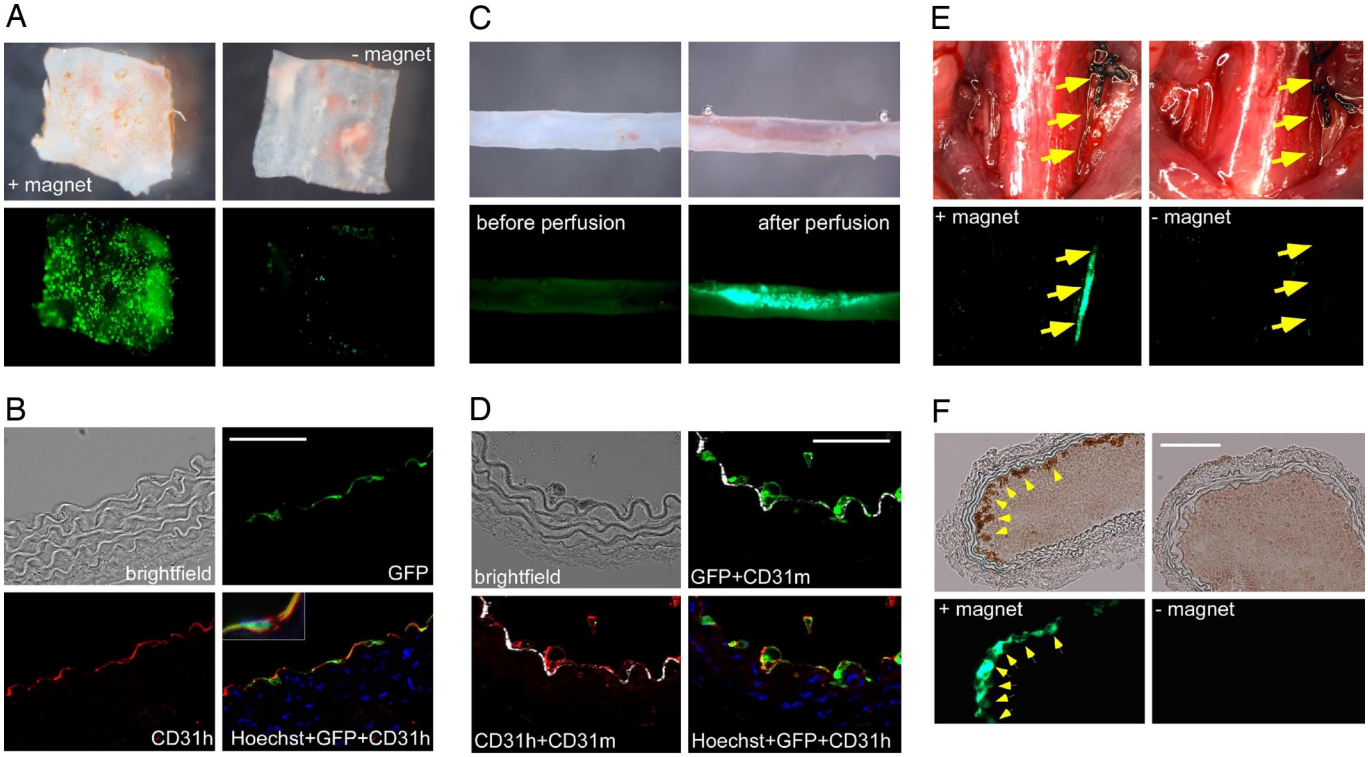


**Fig. 4.** Ex vivo and in vivo positioning of HUVECs to the vessel walls in the presence of hydrodynamic forces or blood flow. (*A*) LV/TM-transduced HUVECs were transferred to aortic strips and cultured for 24 h with (+magnet) and without (-magnet) magnets below the strips while being shaken. Shown are brightfield (*Upper*) and fluorescence pictures (*Lower*) taken by a stereomicroscope (4-fold magnification). (*B*) Immunhistochemical analysis of aortas with LV/TM-transduced HUVECs. Sections were stained with antibodies against human PECAM-1 (CD31h, red) and Hoechst dye (blue). Note the colocalization of the HUVEC-derived CD31h signals with the EGFP fluorescence. The inset shows a triple-stained cell (Hoechst plus eGFP plus CD31h). (*C*) Aortas were perfused ex vivo with medium containing LV/TM-transduced HUVECs while 2 magnets were positioned at one side. Brightfield (*Upper*) and fluorescence images (*Lower*) were taken before and directly after perfusion (3.2-fold magnification). Note the accumulation of EGFP-expressing ''magnetic'' cells. (*D*) Immunhistochemical analysis of the aorta after ex vivo perfusion. Sections were stained with antibodies against murine (CD31m, white) and human CD31 (CD31h, red), and Hoechst dye (blue). Note that EGFP and CD31h signals, which are both derived from the transduced HUVECs, were colocalized and located in close proximity to the murine aortic endothelial layer (CD31m). (*E*) In vivo positioning of LV/TM-transduced HUVECs to the intima of injured common carotid arteries by magnetic forces (+magnet). Control experiments were performed under the same conditions, but without placing a magnet (-magnet). Images were taken 10 min after application of the cells and restoration of the blood flow. Yellow arrows indicate retention of MNP-labeled HUVECs in the area of the magnetic field (*Left*), but not in the control animal (*Right*). Shown are bright-field (*Upper*) and fluorescence images (*Lower*) taken by a stereomicroscope (1.8-fold magnification). (*F*) Histological analysis of the carotid arteries. After application of a magnetic field to the injured common carotid artery, accumulation of MNP-loaded cells was found at the vessel wall (*Left*). No cells were found in the control vessel (*Right*). Shown are bright-field (*Upper*) and fluorescence (*Lower*) pictures. (Scale bars: 50 $\mu$m.)

## Discussion

Targeted delivery of viral vectors could greatly enhance their therapeutic potential because of higher specificity and reduction of side effects. Previous data demonstrated that adsorption of viral and nonviral vectors to cells can be enhanced by nanoparticles (6–8). However, because these experiments were performed under standard cell culture conditions (at 37 °C), it was not clear whether this procedure could be used for the transduction of cells—or even tissues and whole organs—under nonpermissive conditions, such as hydrodynamic forces and shear stress induced by blood flow, as well as hypothermia. Using LV/MNP complexes we were able to overcome the inhibitory effects of these nonpermissive conditions on LV infection. MNPs can be basically distinguished according to their surface charge. The interactions between negatively charged viruses with like-charged MNPs have been shown to be dependent on the presence of divalent counterions, like calcium (6). Positively charged MNPs should directly build up strong interactions with the negatively charged viruses. Our study demonstrates that both types of MNPs exhibited similar LV-binding capacity and that positively as well as negatively charged nanoparticles enhance lentiviral transduction under nonpermissive conditions. In all cells analyzed, MNP-assisted transductions achieved comparable levels of transgene expression to standard overnight LV infections. Importantly, we developed a clinically relevant model for the efficient transduction of endothelial cells under physiological flow conditions by targeting LV/MNP complexes via magnetic forces to the luminal surface of aortas during ex vivo perfusion. Our data clearly demonstrate that MNP-assisted lentiviral transduction results in efficient site-directed targeting of the endothelium, indicating that this method has the potential for localized gene therapy in the vascular system. Furthermore, using external magnets we were able to alter the biodistribution of systemically administered MNP-coupled LVs, indicating that organ-specific targeting can be achieved by using magnetic forces in vivo.

An important aspect of our study is the combination of targeted delivery of viral vectors with positioning of the transduced cells by using superparamagnetic nanoparticles. Cell positioning is of high relevance for regenerative medicine because cell replacement therapies require the efficient seeding of cells in the diseased organs. Especially, systemically delivered cells must establish contact with the target site and overcome hydrodynamic and shear forces generated by the blood flow until more permanent engraftment is achieved. The uptake of MNPs renders cells superparamagnetic, which can be used to capture

MNP-loaded cells by using magnetic forces (9–11). In addition, we reasoned that for many applications, genetic engineering of the cells before transplantation is required; for example, to enhance the therapeutic effect by expressing a therapeutic gene in the transplanted cells. Thus, the transplanted cells function also as vehicles for gene transfer. Here, we studied whether LV/MNP-transduced transgenic cells can be targeted to distinct areas of a blood vessel by magnetic forces. This differs from previous studies, where magnetic forces were used to capture and retain magnetically labeled cells on nonphysiological substrates—that is, stents (10) and Dacron or polytetrafluoroethylene grafts (9, 18). Our data show that MNP-assisted positioning of human endothelial cells can be achieved not only in vessels that were subjected to physiological flow (ex vivo perfusion model), but also in different murine vessels in vivo. Importantly, magnetic cell positioning to the vessel wall was achieved at sites of arterial injury in vivo. These experiments in mice suggest that MNP-based cell positioning might have potential for the development of cell-based therapies aiming at the repair of focal endothelial damage. This strategy appears to be interesting also for cell replacement approaches in other organs, like the heart, because it enables systemic delivery of the cells without invasive surgery and magnet-based, site-restricted positioning. Interestingly, positioning of a relatively low number of cells can have therapeutic effects; for example, the stable engraftment of only a few thousand cardiac progenitors or transgenic skeletal myoblasts strongly reduces the incidence of ventricular arrhythmias after myocardial infarction (19). Taken together, MNP-assisted lentiviral gene transfer and cell positioning is a promising method for combined gene and cell replacement therapies.

## Materials and Methods

All animal experiments were performed in accordance with National Institutes of Health animal protection guidelines and were approved by the local authorities of the University of Bonn.

**MNP-Assisted Lentiviral Transduction of Cells.** CM and TM nanoparticles were obtained from Chemicell. The standard LV/MNP mixture contained a relative amount of ≈50 LVs per cell and ≈27.6 pg of MNPs per virus particle (equal to ≈1,380 pg of MNPs per cell).

**MNP-Assisted Lentiviral Transduction of Aortas.** In a total volume of 800 $\mu$L of HBSS, 52.5 $\mu$g of MNPs were incubated with $\approx 1 \times 10^8$ LVs for 20 min at room temperature. Then, the mixture was applied to the wells, and an NdFeB magnet was placed under the aortas.

**Ex Vivo Perfusion of Mouse Aortas.** A total of 33.75 $\mu$g of MNPs was mixed with $1.7 \times 10^8$ LVs in a total volume of 800 $\mu$L of HBSS and incubated for 20 min at room temperature. During perfusion, 2 small NdFeB magnets were placed in close proximity to one side of the aorta (Fig. 2*A*).

**Magnetic Positioning of HUVECs.** LV/MNP-transduced HUVECs were transferred to 6-well plates and placed onto an aluminum plate containing magnets at defined positions (Fig. S1). For the positioning of HUVECs to vessels, small aortic squares were previously pinned onto the plates. The complete setup was placed onto a compensator (at 5% $CO_2$) and cultured overnight while being shaken slowly (20 rpm). For the positioning of HUVECs to vessels by ex vivo perfusion, LV/TM-transduced HUVECs were introduced into the perfusion system.

**Additional Methods.** A more detailed description of the methods is provided in the *SI Materials and Methods*.

**ACKNOWLEDGMENTS.** We thank Barbara Müller (Department of Virology, Universitätsklinikum Heidelberg, Heidelberg, Germany) for providing the plasmids pCHIV(Env-) and pCHIV.eGFP(Env-). We are very grateful to Christina Stichnote, Jutta Mülich, Frank Holst, and Monika Czechowski for expert technical assistance. This work was supported by the Deutsche Forschungsgemeinschaft Transregio Research Unit 535, the Germany Federal Ministry of Education and Research (FKZ 13N9150), and the NRW International Graduate Research School.

1. Verma IM, Weitzman MD (2005) Gene therapy: Twenty-first century medicine. *Annu Rev Biochem* 74:711–738.
2. Wiznerowicz M, Trono D (2005) Harnessing HIV for therapy, basic research and biotechnology. *Trends Biotechnol* 23:42–47.
3. Dimitrov DS (2004) Virus entry: Molecular mechanisms and biomedical applications. *Nat Rev Microbiol* 2:109–122.
4. Marsh M, Helenius A (2006) Virus entry: Open sesame. *Cell* 124:729–740.
5. Smith AE, Helenius A (2004) How viruses enter animal cells. *Science* 304:237–242.
6. Haim H, Steiner I, Panet A (2005) Synchronized infection of cell cultures by magnetically controlled virus. *J Virol* 79:622–625.
7. Scherer F, *et al.* (2002) Magnetofection: Enhancing and targeting gene delivery by magnetic force in vitro and in vivo. *Gene Ther* 9:102–109.
8. Kadota S, *et al.* (2005) Enhancing of measles virus infection by magnetofection. *J Virol Methods* 128:61–66.
9. Pislaru SV, *et al.* (2006) Magnetic forces enable rapid endothelialization of synthetic vascular grafts. *Circulation* 114:I314–I318.
10. Pislaru SV, *et al.* (2006) Magnetically targeted endothelial cell localization in stented vessels. *J Am Coll Cardiol* 48:1839–1845.
11. Shimizu K, *et al.* (2007) Effective cell-seeding technique using magnetite nanoparticles and magnetic force onto decellularized blood vessels for vascular tissue engineering. *J Biosci Bioeng* 103:472–478.
12. Eberbeck D, Wiekhorst F, Steinhoff U, Trahms L (2006) Aggregation behaviour of magnetic nanoparticle suspensions investigated by magnetorelaxometry. *J Phys Condens Matter* 18:S2829–S2846.
13. Lampe M, *et al.* (2007) Double-labelled HIV-1 particles for study of virus-cell interaction. *Virology* 360:92–104.
14. Pan D, *et al.* (2002) Biodistribution and toxicity studies of VSVG-pseudotyped lentiviral vector after intravenous administration in mice with the observation of in vivo transduction of bone marrow. *Mol Ther* 6:19–29.
15. Butler SL, Hansen MS, Bushman FD (2001) A quantitative assay for HIV DNA integration in vivo. *Nat Med* 7:631–634.
16. Pfeifer A, *et al.* (2006) Lentivector-mediated RNAi efficiently suppresses prion protein and prolongs survival of scrapie-infected mice. *J Clin Invest* 116:3204–3210.
17. Lindner V, Fingerle J, Reidy MA (1993) Mouse model of arterial injury. *Circ Res* 73:792–796.
18. Perea H, *et al.* (2007) Vascular tissue engineering with magnetic nanoparticles: seeing deeper. *J Tissue Eng Regen Med* 1:318–321.
19. Roell W, *et al.* (2007) Engraftment of connexin 43-expressing cells prevents post-infarct arrhythmia. *Nature* 450:819–824.